THE JOURNAL OF BIOLOGICAL CHEMISTRY VOL. 290, NO. 13, pp. 8447–8456, March 27, 2015

Functional Significance of Point Mutations in Stress Chaperone Mortalin and Their Relevance to Parkinson Disease*

Received for publication, November 19, 2014, and in revised form, January 21, 2015 Published, JBC Papers in Press, February 2, 2015, DOI 10.1074/jbc.M114.627463

Renu Wadhwa[‡1], Jihoon Ryu[‡§1], Hyo Min Ahn[‡§], Nishant Saxena[‡], Anupama Chaudhary[‡], Chae-Ok Yun[§2], and Sunil C Kaul[‡3]

From the [‡]Cell Proliferation Research Group and Department of Biotechnology (DBT, India)-National Institute of Advanced Industrial Science and Technology (AIST, Japan) International Laboratory for Advanced Biomedicine (DAILAB), Tsukuba, Ibaraki 305-8562, Japan and the [§]Department of Bioengineering, College of Engineering, Hanyang University, 222 Wangsimni-Ro, Seongdong-Gu, Seoul 133-791, Korea

Background: Mortalin, an essential chaperone, is enriched in cancers; it possesses pro-proliferative and anti-apoptotic functions and has been found mutated in some Parkinson patients.
Results: Mutant mortalins lack functions involved in carcinogenesis and cause increased oxidative stress; we demonstrate the factors and mechanism of their role in Parkinson disease.
Conclusion: Mutations in mortalin contribute to Parkinson disease.
Significance: This work contributes toward an understanding of mortalin-associated diseases for therapy.

Mortalin/mtHsp70/Grp75 (mot-2), a heat shock protein 70 family member, is an essential chaperone, enriched in cancers, and has been shown to possess pro-proliferative and anti-apoptosis functions. An allelic form of mouse mortalin (mot-1) that differs by two amino acids, M618V and G624R, in the C terminus substrate-binding domain has been reported. Furthermore, genome sequencing of mortalin from Parkinson disease patients identified two missense mutants, R126W and P509S. In the present study, we investigated the significance of these mutations in survival, proliferation, and oxidative stress tolerance in human cells. Using mot-1 and mot-2 recombinant proteins and specific antibodies, we performed screening to find their binding proteins and then identified ribosomal protein L-7 (RPL-7) and elongation factor-1 α (EF-1α), which differentially bind to mot-1 and mot-2, respectively. We demonstrate that mot-1, R126W, or P509S mutant (i) lacks mot-2 functions involved in carcinogenesis, such as p53 inactivation and hTERT/hnRNP-K (heterogeneous nuclear ribonucleoprotein K) activation; (ii) causes increased level of endogenous oxidative stress; (iii) results in decreased tolerance of cells to exogenous oxidative stress; and (iv) shows differential binding and impact on the RPL-7 and EF-1α proteins. These factors may mediate the transformation of longevity/pro-proliferative function of mot-2 to the premature aging/anti-proliferative effect of mutants, and hence may have significance in cellular aging, Parkinson disease pathology, and prognosis.

Aging is an innate multifactorial process that leads to functional deterioration of living systems over time and ends with death. The mortality of an organism is largely considered as an outcome of accumulation of structural and functional errors that gradually trigger senescence (1). Although the exact players that limit the lifespan of normal cells are not completely known, it is generally accepted that cellular aging or senescence is a signal transduction program that induces an irreversible growth arrest state in normal cells. Tumor suppressor pathways (p53 and/or retinoblastoma protein and their regulators, such as $p16^{INK4a}$, $p21^{WAF1}$, and $p14^{ARF}$) have been established to play critical roles in cellular senescence (2–4). What activates these gene functions is not fully understood. One likely candidate is DNA damage, particularly at chromosome ends, that is generated spontaneously with each cell division in the form of attrition of the telomeres (5, 6). DNA damage and oxidative stress-related signaling have recently been linked not only to cellular aging/replicative senescence but also to the age pathologies including Parkinson and Alzheimer diseases (7–9). Protein modifications, *e.g.* the oxidation, glycation, and deamidation of asparaginyl and glutaminyl residues, the formation of isopeptide bonds, and the accumulation of molecular damage, have been reported to contribute to cellular and organismal aging. Interestingly, tissue susceptibility to experimentally induced protein modification not only depends on tissue type and age, but also on the maximum lifespan potential of species (1, 10). Accumulation of misfolded proteins is especially pronounced in aged cells. Hence they heavily depend on their innate "proteotoxic surveillance" provided by ubiquitous molecular chaperones, the heat shock proteins. Chaperones are necessary to regulate various cellular signaling processes and

* This study was partly supported by grants-in-aid for scientific research (Kakenhi) from the Japanese Society for the Promotion of Science, Japan (to S. C. K.) and grants from the Korea Food and Drug Administration (13172KFDA306) and the Korea Science, Engineering Foundation (2010-0029220, 2013K1A1A2A02050188, 2013M3A9D3045879, brain Korea 21 plus) (to C. O. Y.)
[1] Both authors contributed equally to this work.
[2] To whom correspondence should be addressed: Dept. of Bioengineering, College of Engineering, Hanyang University, 222 Wangsimni-Ro, Seongdong-gu, Seoul, Korea. Tel.: 82-2-2220-0491; Fax: 82-2-2220-4850; E-mail: chaeok@hanyang.ac.kr.
[3] To whom correspondence should be addressed: National Institute of Advanced Industrial Science and Technology (AIST), Central 4, 1-1-1 Higashi, Tsukuba, Ibaraki 305-8562, Japan. Tel.: 81-29-86713; Fax: 81-29-861-2900; E-mail: s-kaul@aist.go.jp.

prevent deleterious age-associated accumulation of protein aggregates (11, 12). Although a high degree of complex aggregates is found in the post-mitotic neurons with age-related neurodegenerative diseases (Alzheimer, Parkinson, and Huntington diseases, etc.), the induction of Hsps[4] has been shown to counteract the aging process. This may be one reason why long-lived species and immortal cells constitutively express Hsps (13, 14).

The heat shock protein 70 family (Hsp70) family member mortalin (also called mtHsp70/Grp75/PBP74) was first identified as "mot-1/mortality factor" in cytoplasmic extracts of senescent murine fibroblasts and mortal mouse cell hybrids (15). It induced cellular senescence in NIH 3T3 cells (16). In contrast, overexpression of mortalin-2 (mot-2) protein (differs by only two amino acids in the C terminus; V618M and R624G) caused malignant transformation of immortalized mouse fibroblast and enhanced longevity of *in vitro* human fibroblasts (17, 18). Knocking in extra copies of a *Caenorhabditis elegans* homologue of mot-2 caused increase in their lifespan (19). These effects have been ascribed, in part, to the ability of mot-2 to (i) inactivate wild-type p53 functions including transcriptional activation (20, 21), control of centrosome duplication (22), and deregulation of apoptosis in cancer cells (23–25); (ii) activate telomerase and hnRNP-K (26); (iii) and regulate oxidative stress (27, 28) and mitochondrial structure (29, 30). On the other hand, deficiency in mortalin has been well connected to the age-related pathologies including Alzheimer and Parkinson diseases (28, 31–33). Genomic studies have identified mutants of mortalin in PD patients from Swedish and German populations (31, 32). In light of this information and to resolve the functional significance of these mutants in aging and age pathologies, we generated human cells expressing mot-1 or mortalin-PD (mot-PD) mutant proteins. We demonstrate that in contrast to the role of mot-2 in cancer phenotype, these proteins cause growth arrest of cells by different signaling pathway.

EXPERIMENTAL PROCEDURES

Cell Culture—Human osteosarcoma (U2OS), lung adenocarcinoma (A549), neuroblastoma (IMR32), and rat glioblastoma (C6) were maintained in DMEM (Gibco BRL), and melanoma (G361) was maintained in McCoy's 5A medium (Gibco BRL) containing 10% fetal bovine serum (Gibco BRL) and 1× antibiotic-antimycotic (Gibco BRL). Cells were procured from the Japanese Collection of Research Bioresources (JCRB) Cell Bank, National Institute of Biomedical Innovation, Osaka, Japan (A549, IMR32, and G361), DS Pharma Biomedical Co. Ltd., Osaka, Japan (U2OS), and Cell Resource Center for Biomedical Research, Institute of Development Aging and Cancer, Tohoku University, Japan (C6).

Construction of Retroviral Vectors and Derivative Cell Lines—Full-length mot-1, mot-2 (15, 16), and point-mutated mortalins found in Parkinson disease patients (R126W and P509S) (32) were generated by PCR and cloning into the HindIII site of the pCX4neo vector. All the constructs coded for full-length proteins containing signal peptide sequence. They harbored the following amino acid alterations at 624, 618, 509, and 126 residues: mot-1, RVPR; and mot-2, GMPR, GMPW, and GMSR, respectively. Retroviruses were produced in Plat-E cells. The stably infected cells were maintained in 100 μg/ml G418-supplemented medium.

Recombinant Protein Expression and Purification—Escherichia coli M15 cells were transformed with the expression constructs pET16/mot-1 and pET16/mot-2 and cultured at 37 °C until A_{600} read 0.5–0.7. Isopropyl-1-thio-β-D-galactopyranoside was added to a final concentration of 1 mM, and cells were further cultured for 5 h. Bacteria were harvested by centrifugation and lysed by sonication in Buffer A (100 mM NaH_2PO_4; 10 mM Tris-HCl, pH 9.0; 8 M urea; 10 mM β-mercaptoethanol; 15 mM imidazole). The lysate was centrifuged at 20,000 × *g* for 20 min, and the soluble fraction was used for purification using nickel nitrilotriacetic acid-agarose beads (Ni-NTA-agarose) (Qiagen, Inc.). Lysate from the bacteria expressing mot-1 or mot-2 proteins was incubated with the beads placed in a column followed by washing three times with buffer (100 mM NaH_2PO_4; 10 mM Tris-HCl, pH 5.9; 8 M urea; 10 mM β-mercaptoethanol; 0.1% Triton X-100). Recombinant mortalin proteins were eluted with the wash buffer followed by Buffer B (100 mM NaH_2PO_4; 10 mM Tris-HCl, pH 4.5; 8 M urea; 10 mM β-mercaptoethanol). The eluted proteins were dialyzed for 48 h against 20 mM Tris-HCl, pH 7.8; 150 mM NaCl; and 10 mM β-mercaptoethanol. Proteins were concentrated by lyophilization and quantified using the Bio-Rad protein assay kit (Bio-Rad) with bovine serum as standard. The proteins were separated by SDS-PAGE and analyzed by Western blot using antibodies as indicated.

Protein Pulldown Assays and MALDI—Recombinant proteins were mixed with cell lysate from U2OS cells and were incubated at 4 °C for 12–24 h. Proteins were pulled down with either Ni-NTA agarose or anti-mortalin antibody. The protein complexes were washed with NP-40 lysis buffer (15) three times, resolved in SDS-polyacrylamide gel, and stained with Coomassie Brilliant Blue. Bands of interest were excised from the gel and processed for Matrix-assisted laser desorption/ionization MALDI analysis.

Cell Proliferation Rate and Oxidative Stress Response—Cell proliferation was measured by the 3-(4,5-dimethylthiazol-2-yl)-2,5-diphenyltetrazolium bromide (MTT) assay (Invitrogen) using 96-well plates (10^3 cells/well). For oxidative stress, cells were treated with 1.0 mM hydrogen peroxide (2 h) followed by recovery in the fresh medium (48–72 h). Cells were incubated with 100 μl of MTT solution (0.5 mg/ml) for 4 h at 37 °C. The solution was removed, and 100 μl of dimethyl sulfoxide (DMSO) were added to each well. The absorbance was measured at 570 nm, using a microplate reader (Infinite 200 PRO; Tecan Group Ltd.). All assays were performed independently at least three times.

Colony-forming Assay—Cells (1×10^3) were seeded on 6-well plates. Cells were maintained until the appearance of colonies with regular change of medium. Colonies were fixed in metha-

[4] The abbreviations used are: Hsp, heat shock protein; PD, Parkinson disease; RPL-7, ribosomal protein L-7; EF-1α, elongation factor 1-α; hnRNP-K, heterogeneous nuclear ribonucleoprotein K; mot, mortalin; mot-F, full-length mortalin; ROS, reactive oxygen species; Ni-NTA, nickel-nitrilotriacetic acid; TRAP, telomere repeat amplification protocol.

nol, stained with 0.5% crystal violet, photographed, and counted.

Detection of Reactive Oxygen Species—Cells were cultured on glass coverslips placed in 12-well plates and stained for reactive oxygen species (ROS) by fluorescent staining using the Image-iT™ LIVE Green ROS detection kit (Molecular Probes, Eugene, OR). Images were captured on a Zeiss Axiovert 200M microscope and analyzed by AxioVision 4.6 software (Carl Zeiss Microimaging, Thornwood, NY).

Western Blotting—Cells were lysed with radioimmunoprecipitation assay buffer (Thermo Scientific) containing complete protease inhibitor cocktail (Roche Applied Science, Mannheim, Germany). Cell lysates were separated on a SDS-polyacrylamide gel and transferred onto PVDF membranes that were incubated with antibodies against mortalin (polyclonal: R-antibody, S-antibody, and monoclonal: 37-6 clone), Myc tag, hnRNP-K, elongation factor 1-α (EF-1α), eIF2α, and eEF2 (Cell Signaling, Danvers, MA); p53 (Santa Cruz Biotechnology, Santa Cruz, CA); and ribosomal protein L-7 (RPL-7) and actin (Abcam, Cambridge, UK) as indicated. Protein bands were detected by chemiluminescence (GE Healthcare, Buckinghamshire, UK) using a LAS3000-mini (Fuji Film, Tokyo, Japan) through horseradish peroxidase-conjugated secondary antibodies (Santa Cruz Biotechnology).

Immunostaining—Cells were plated on coverslips placed in the 12-well culture plates. They were fixed with chilled fixing solution of methanol-acetone (1:1) for 10 min prior to incubate with primary antibodies (p53 and Myc, Santa Cruz Biotechnology; Myc tag, Cell Signaling; or mortalin (20)) at 4 °C overnight followed by extensive washings in PBS-T (PBS with 0.2% Triton X-100) and incubation with the fluorochrome-conjugated secondary antibodies (Alexa Fluor 488-conjugated goat anti-rabbit or anti-mouse or Alexa Fluor 594-conjugated goat anti-rabbit or anti-mouse (Molecular Probes) as described (20)). Stained cells were examined on a Zeiss Axiovert 200M microscope and analyzed by AxioVision 4.6 software (Carl Zeiss). Images were quantified by ImageJ software (National Institute of Health, Bethesda, MD). To examine the presence of mortalin in nucleus, images were acquired with a laser scanning confocal microscope (Zeiss LSM 700). The files were transferred to a graphic workstation and analyzed with Imaris software (Bitplane, Zurich, Switzerland).

p53-dependent Reporter Assays—Control, mot-1, and mot-2 cells (1×10^5/well) were plated in 6-well plates and transfected with 1 μg of pGL13-luc plasmid vector containing firefly luciferase gene- and p53-responsive elements. pRL-TK (Promega, Madison, WI) vector was used as transfection efficiency control. Cells were lysed, and luciferase activity was measured using the Dual-Luciferase reporter assay system (Promega) and a microplate reader (Infinite 200 PRO; Tecan Group Ltd.).

Telomere Repeat Amplification Protocol (TRAP) Assay—TRAP assay (for semiquantitative detection of telomerase activity) was performed using the *TeloTAGGG* telomerase PCR ELISA kit (Roche Applied Science, Mannheim, Germany). Cell lysates were prepared in lysis reagent from cultured (2×10^5) cells. The supernatant collected after centrifugation at $16{,}000 \times g$ for 20 min at 4 °C was used for TRAP assay. Telomerase activity in the sample was calculated as units of activity relative to the positive control. Heat-inactivated G361 lysate was used as negative control. All the assays were performed in triplicate.

Statistical Analysis—The data are expressed as a means ± S.E., and the significance of differences between groups was determined by the Mann-Whitney test (nonparametric rank sum test) using StatView software (Abacus Concepts, Inc., Berkeley, CA). Differences were considered significant when $p < 0.05$.

RESULTS AND DISCUSSION

mot-1 and mot-2 Cause Contrasting Effects on Cell Proliferation—Retrovirus-mediated exogenous expression of Myc-tagged mot-1 (Val-618 and Arg-624) and mot-2 (Met-618 and Gly-624) in U2OS, G361, and IMR32 (human) and C6 (rat) cells revealed morphological differences. Although mot-2 derivatives appeared more rounded and smaller as compared with the control cells, the mot-1 derivatives showed elongated and flattened morphology (Fig. 1*A* and data not shown) in all these cell types. Cell proliferation/growth rate analyses showed that mot-1 and mot-2 derivatives divided more slowly and more quickly than the control cells, respectively (Fig. 1*B*). Long term colony-forming assays also revealed similar phenotype in all the cell lines. As compared with the control cells, mot-1 derivatives formed smaller and fewer colonies, and the mot-2 derivatives formed bigger and more colonies (Fig. 1*C* and data not shown). We isolated several mot-1 and mot-2 derivative clones of U2OS cells. The level of expression of mot-1 and mot-2 proteins was examined by Western blotting with anti-Myc and anti-mortalin antibodies. Cell proliferation assays of these clones revealed that although mot-2 accelerated the growth of parent U2OS cells, mot-1 caused their growth inhibition (Fig. 1*D*). Furthermore, dose-dependent inhibition of growth was observed in mot-1-transduced human lung fibroblasts (A549) and melanoma cells (G361) and rat glioblastoma (C6) cells (data not shown), demonstrating that the anti-proliferative effect of mot-1 was not cell line- or species-specific.

mot-1 Lacks Transforming Activity of mot-2—mot-2 has been shown to cause pro-proliferative effect and malignant transformation of human cancer cells by inactivation of p53 functions, including transcriptional inactivation (34), control of centrosome duplication (22), and deregulation of apoptosis (23, 24) in cancer cells. Most recently, we reported that the nuclear mot-2 activates telomerase and hnRNP-K and contributes to cancer aggressiveness (26). In light of these findings, we investigated the capability of mot-1 in these assays. As shown in Fig. 2, *A* and *B*, immunolocalization of transfected mot-1 and mot-2 proteins by anti-Myc tag antibody revealed nuclear staining of mot-2/Myc; mot-1 was not found in the nucleus. Similar results were obtained in mot-1 and mot-2 derivatives of G361 and C6 cells (data not shown).

We next examined the expression of p53 and its activity level in mot-1 and mot-2 derivatives of U2OS and G361 cells. As shown in Fig. 3, *A–C*, consistent with earlier studies, p53 protein as well as its transcriptional activation function decreased in mot-2-overexpressing cells. In contrast, there was no decrease in the level of p53 in mot-1 derivatives. Instead, increase in nuclear p53 and p53-dependent reporter assays was

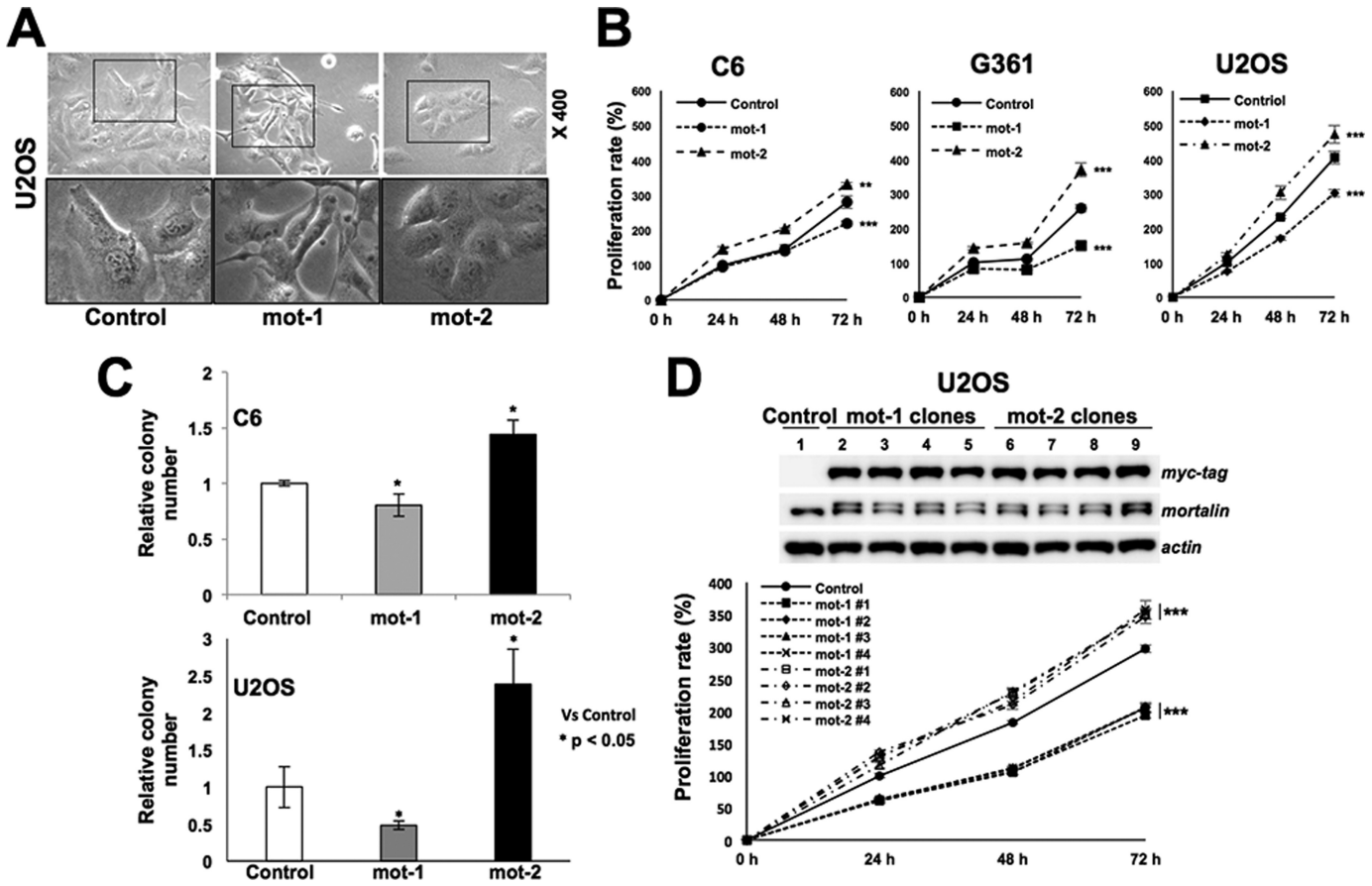

FIGURE 1. **mot-1 and mot-2 proteins cause contrasting effects on cell proliferation.** *A–C*, morphology (*A*), relative proliferation (*B*), and colony-forming efficacy (*C*) of the indicated cells transduced with mot-1- or mot-2-encoding retroviruses. *D*, expression level of Myc-tagged mortalins and proliferation analyses of mot-1 and mot-2 derivatives of U2OS cells showing, as compared with the control, increased rate of proliferation in all the mot-2 derivatives; mot-1 derivatives proliferated slowly. The data are expressed as a means ± S.E. ***, $p \leq 0.001$.

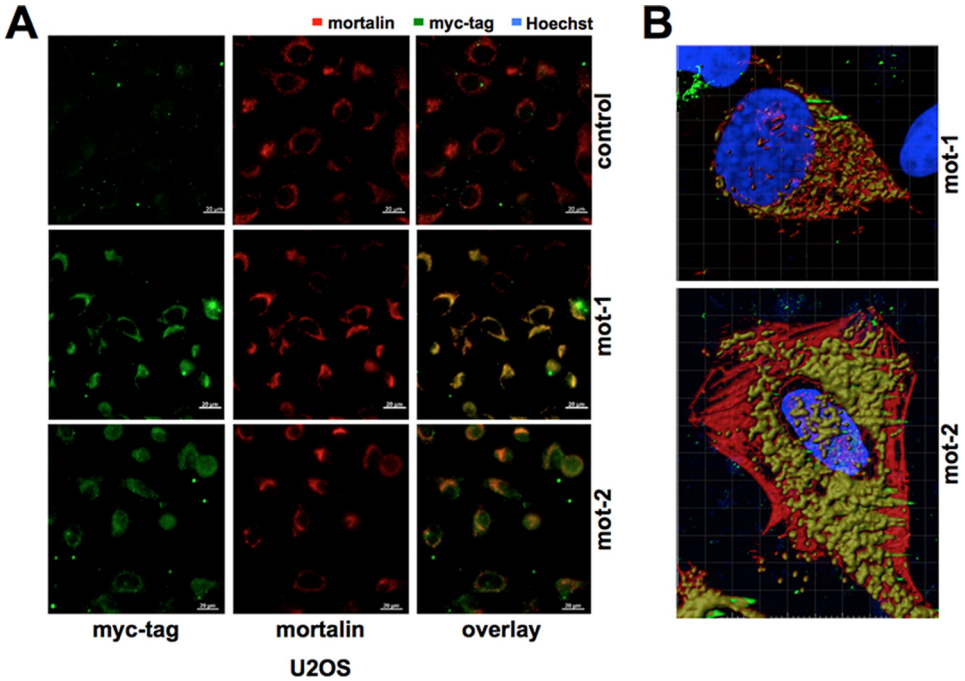

FIGURE 2. **mot-2, but not mot-1, localizes in the nucleus.** *A*, double immunostaining of mot-1- and mot-2-transduced U2OS cells with anti-Myc and anti-mortalin antibodies showing nuclear staining only in mot-2 Myc cells. *B*, high-resolution imaging of cells transduced with Myc-tagged mortalins and stained for endogenous mot-2 (*red*) and exogenous mot (*green*) showing the absence of mot-1 in the nucleus. Images were acquired with a confocal laser scanning microscope. Nucleus was stained with Hoechst 33342 (*blue*) and was made transparent to show the existence of mortalin in the nucleus with Imaris software.

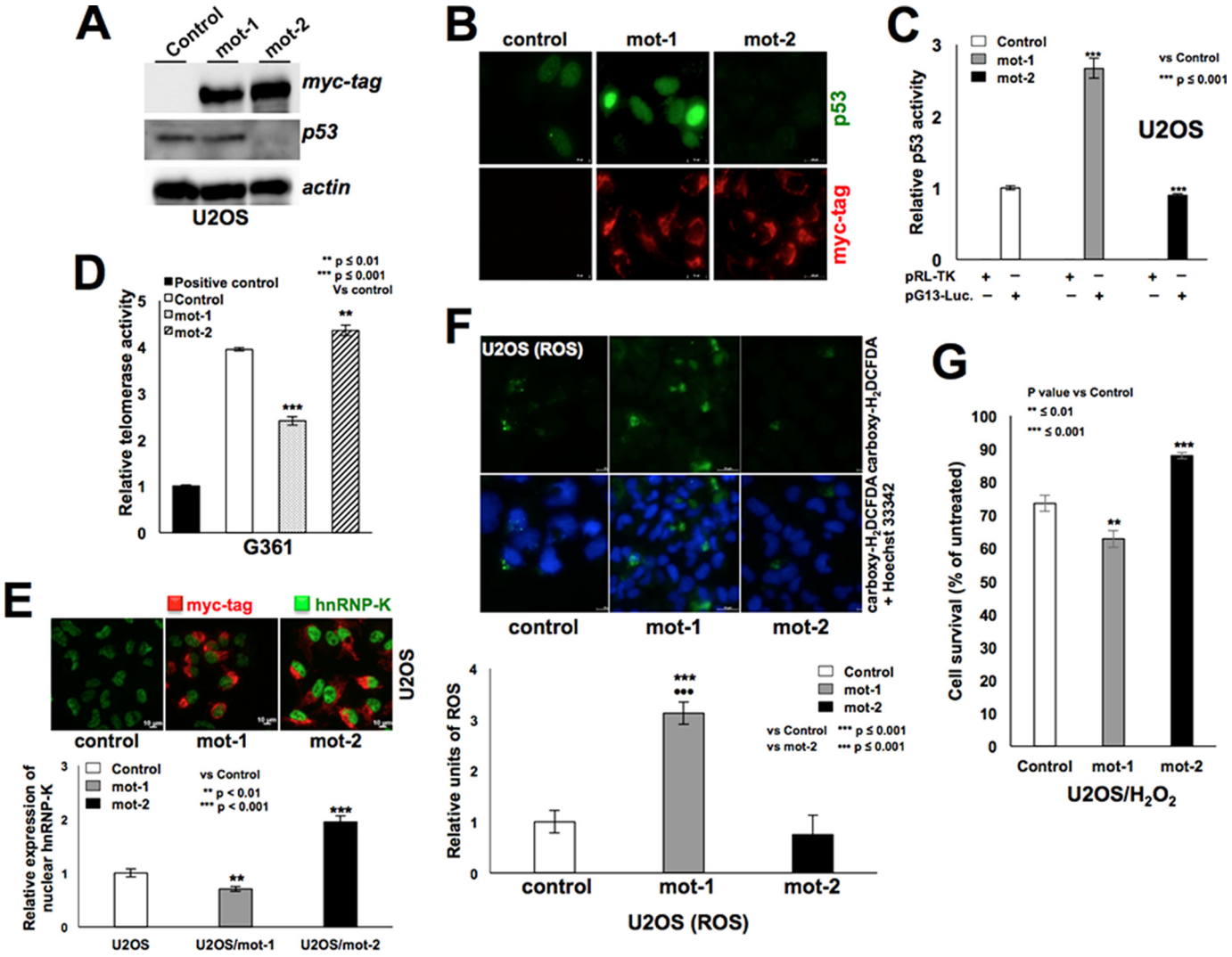

FIGURE 3. **mot-1 lacks cell-transforming activities like that of mot-2.** *A–C*, mot-2-transduced cells showing decrease in the level, nuclear localization, and transcriptional activation function of p53. The level of p53 in mot-1-transduced cells remained unchanged (*A*), showed enrichment in nucleus (*B*), and showed increase in transcriptional activation function in mot-1-transduced cells (*C*). *D*, telomerase activity decrease in mot-1-transduced cells, in contrast to increase in mot-2-transduced cells. *E*, mot-2-transduced, but not mot-1-transduced, cells showed enrichment of nuclear hnRNP-K. Quantitation of cells with bright hnRNP-K fluorescence signal is shown below. *F* and *G*, mot-1-transduced cells showed increase in endogenous ROS (quantitation is shown below) (*F*), and were more sensitive to H_2O_2-induced stress (*G*) than mot-2 cells. *H_2DCFDA*, 2′,7′-dichlorodihydrofluorescein diacetate. The data are expressed as a means ± S.E.

observed (Fig. 3, *B* and *C*). Investigation on the telomerase activity of mot-1 and mot-2 derivatives of G361 (telomerase plus cell line) by TRAP assay showed increase in mot-2 derivatives. Interestingly, mot-1 derivatives showed reduction in the telomerase activity (Fig. 3*D*). Immunocytochemical examination of hnRNP-K showed its nuclear enrichment only in the mot-2 derivatives (Fig. 3*E*). Most noticeably, mot-1 showed a high level of endogenous ROS (Fig. 3*F*) and was more sensitive to H_2O_2-induced stress as compared with the mot-2 derivative cells (Fig. 3*G*). Taken together, these data showed that mot-1 and mot-2 possess distinct activities, and these differences may mediate their contrasting effect on cell proliferation.

Identification and Characterization of mot-1- and mot-2-binding Proteins—To get further insights into the differential activities of mot-1 and mot-2 proteins, we aimed to identify their interacting partners. We generated (i) recombinant His-tagged mot-1 and mot-2 proteins in bacteria and (ii) mot-1- and mot-2-specific antibodies using their peptides as antigens (Fig. 4*A*). Characterization of recombinant mot-1 and mot-2 proteins has earlier revealed their different spectra in intrinsic tryptophan and 8-anilinonaphthalene-1-sulfonic acid (ANS) fluorescence assays, as well as different chaperoning activities in luciferase folding and insulin aggregation assays (35). Reactivity to the antibodies to mot-1 and mot-2 proteins was examined using recombinant proteins. As shown by Western blotting in Fig. 4*B*, antibodies "R" and "S" were specific to mot-1 and mot-2 proteins, respectively.

To identify binding proteins, recombinant mot-1 or mot-2 protein was mixed and incubated with U2OS cell lysate overnight followed by their precipitation with either Ni-NTA-agarose or anti-mortalin antibody (Fig. 4*C*). The precipitates were resolved in parallel lanes on SDS-polyacrylamide gels and stained with SYPRO® Orange (Fig. 4*C*). The protein bands that showed differential binding to either mot-1 or mot-2 were extracted from gel and subjected to MALDI. The analysis revealed the identity of five mot-1-binding proteins, *i.e.* EF-1α,

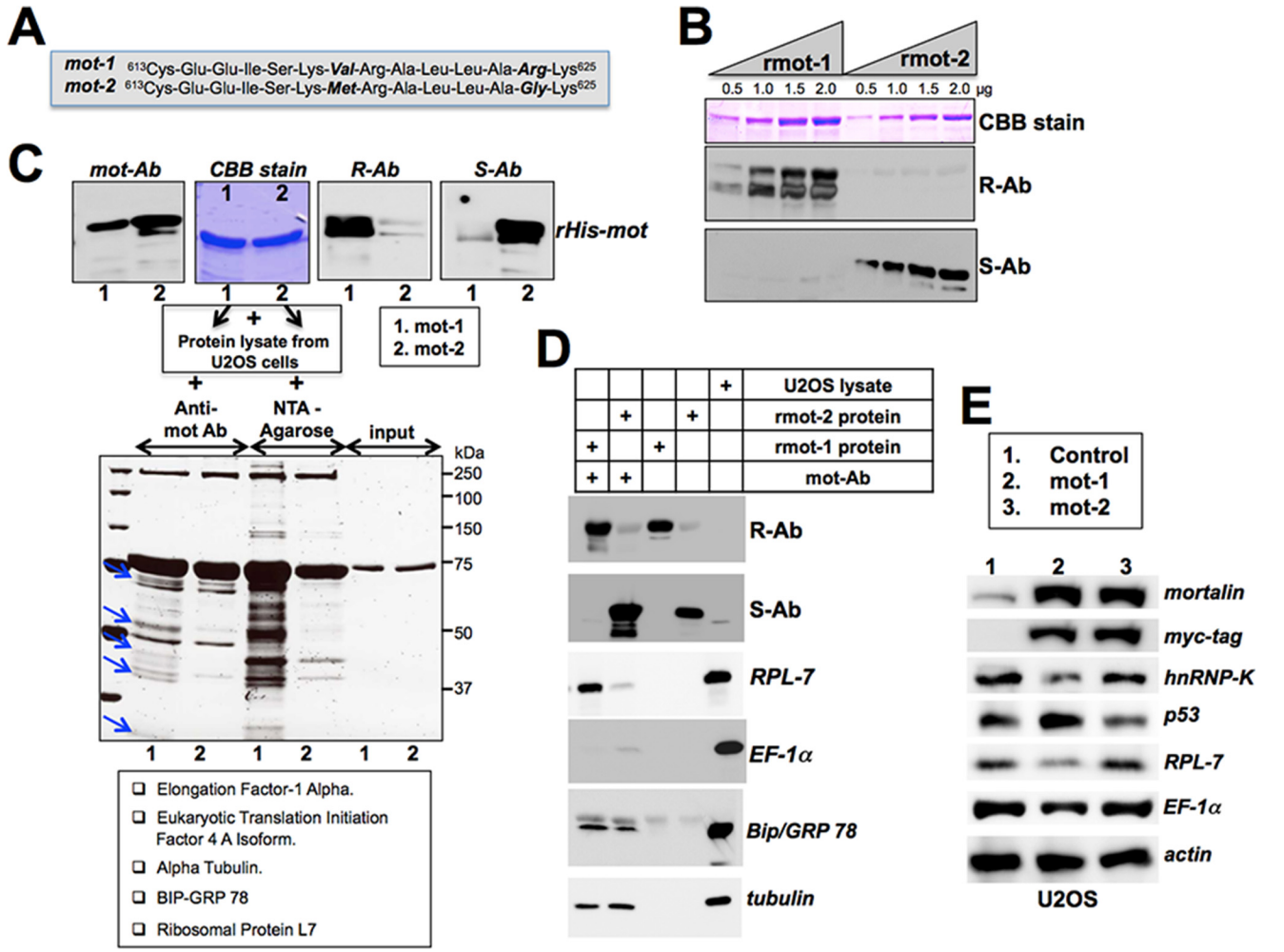

FIGURE 4. **Identification of mot-1- and mot-2-binding proteins.** *A*, sequence of mot-1 and mot-2 peptides used as antigens for raising specific antibodies R and S, respectively. *B*, specificity of R and S antibodies (*R-Ab* and *S-Ab*) to recombinant mot-1 (*rmot-1*) and mot-2 (*rmot-2*) proteins. *CBB stain*, Coomassie Brilliant Blue stain. *C*, identification of mot-1-binding proteins by immunoprecipitation (with anti-mortalin antibody; *Anti-mot Ab*) and pulldown assays (with Ni-NTA-agarose). Proteins showing differential binding with mot-1 are shown by *blue arrows*. *D*, validation of RPL-7 and EF-1α as preferentially binding to mot-1 and mot-2 proteins, respectively. Recombinant mot-1 and mot-2 proteins were incubated with cell lysates followed by immunoprecipitation of the complexes with anti-mortalin antibody. Immunoprecipitated proteins were examined by Western blotting with specific antibodies. RPL-7 and EF-1α showed preferential binding to mot-1 and mot-2, respectively. Grp78 and tubulin did not show difference in binding to either mot-1 or mot-2 protein. *E*, expression analyses of binding proteins in mot-1- or mot-2-transduced cells. Both RPL-7 and EF-1α were decreased only in mot-1-transduced cells. Although hnRNP-K increased in mot-2-transduced cells, p53 decreased in mot-2-transduced cells.

eukaryotic translation initiation factor 4 A isoform, α-tubulin, BIP-GRP 78, and RPL-7 (Fig. 4*C*). We next validated the binding of these proteins by Western blotting of mot-1 and mot-2 immunocomplexes with specific antibodies. As shown in Fig. 4*D*, we found that RPL-7 precipitated predominantly with mot-1. GRP78 and tubulin showed no difference, and EF-1α was found in relatively greater amounts in the mot-2 immunocomplexes. To investigate the effect of mot-1/mot-2 binding on RPL-7 and EF-1α, we next examined their level of expression in respective derivative U2OS cells. As shown in Fig. 4*E*, mot-1 derivatives showed decrease in the expression of RPL-7, EF-1α, and hnRNP-K as compared with control cells. p53, as expected from earlier studies, was decreased in mot-2 derivative cells; mot-1 derivatives showed increase in p53 expression level. Furthermore, elongation factor 2 and elongation factor 2α also showed increase in mot-2 and decrease in mot-1 derivative cells (data not shown).

PD Mutants of Mortalin, R126W, and P509S Mimic mot-1 Functions—Two missense mutations of mortalin have been detected in Parkinson patients (32, 36). In light of the above data on anti-proliferative and oxidative stress impact due to mot-1, we investigated the relevance of PD mutants of mortalin in disease phenotype. Myc-tagged mortalin mutants (R126W and P509S) were generated in the background of human full-length mortalin (also called mot-F) (26) in retrovirus vector similar to mot-1 and mot-2 (Fig. 5*A*). Expression of the mutants was examined by Western blotting with anti-Myc tag antibody (Fig. 5*B*). As shown in Fig. 5*C*, both mutants caused changes in cell morphology and their growth rate similar to the ones observed for mot-1-infected cells (Fig. 1*A*). The mortalin PD mutant derivative cells were elongated, large, and flattened, similar to senescent cells, proliferated more slowly than the control cells (Fig. 5*D*), and had lower colony-forming efficacy (Fig. 5*E*). Similar results were obtained in A549 cells (data not

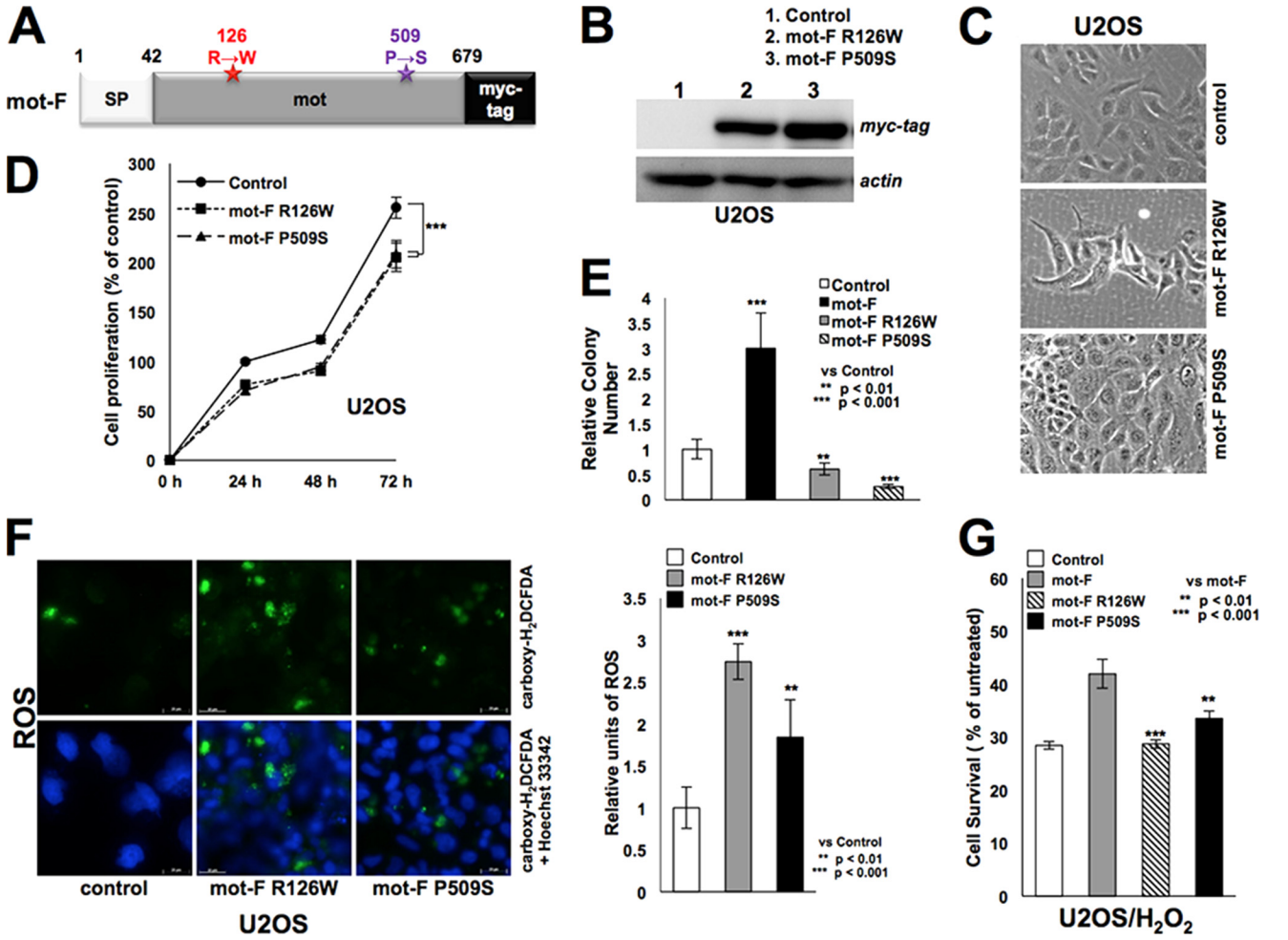

FIGURE 5. **Functional characterization of mortalin PD mutants.** *A*, schematic presentation of mot-PD mutants. *B–E*, morphology of mot-PD mutant (mot-F R126W and mot-F P509S)-transduced U2OS cells and their expression as examined by Western blotting with anti-Myc antibody (*B*). Cells show flattened and enlarged morphology (*C*), slower growth rate (*D*), and lower colony-forming efficacy (*E*) as compared with control- and mot-F-transduced cells. *F* and *G*, mot-PD-transduced cells showed higher endogenous ROS (*F*) and high sensitivity to exogenous (H_2O_2) stress (*G*) as compared with control mot-F-transduced cells. The data are expressed as a means ± S.E. *SP*, signal peptide.

shown). Immunolocalization of the mutant proteins revealed their cytoplasmic localization (data not shown). Most significantly, the mot-PD mutant derivative cells showed high levels of ROS (endogenous stress) (Fig. 5*F*). These cells were also more sensitive to exogenous oxidative stress, determined by increase in H_2O_2-induced ROS, as compared with control mot-F derivatives (Fig. 5*G*). We examined the expression of p53 and hnRNP-K in these cells and found increased nuclear p53 in R126W- and P509S-transduced cells in contrast to the decrease observed in mot-F derivatives (Fig. 6*A*). p53-dependent reporter activity also showed contrasting effects; it decreased in mot-F cells and increased in R126W- and P509S-transduced cells (Fig. 6*B*). Furthermore, although nuclear hnRNP-K increased in mot-F derivatives, R126W- and P509S-transduced cells showed decrease (Fig. 6*C*). Western blotting confirmed these data, showing increase in p53 and decrease in hnRNP-K in mortalin PD mutant-transduced cells, similar to that of mot-1, and in contrast to that of mot-2 and mot-F (Figs. 4*E* and 6*D*). Furthermore, RPL-7, EF-1α, EF-2, and EF-2α showed strong decrease in mortalin PD mutant derivatives (Fig. 6*D*).

The Hsp70 proteins are an important group of molecular chaperones with life-essential and pro-survival roles. They function by preventing protein aggregation, assisting folding/refolding of partially unfolded intermediary structures, and targeting proteins for the degradation machinery, the proteasome. In all these cellular processes, Hsp70s are thought to interact with transiently unraveled segments or globally denatured protein substrates (37). The two murine mortalins differ only by two amino acid residues in the C terminus; in comparison with mot-2, mot-1 has Val instead of Met at position 618, as well as Arg instead of Gly at 624. Furthermore, a comparison of different Hsp70s shows that only mot-1 lacks the canonical bend between helices C and D leading to an aberrant fusion of these two helical subdomains. This would particularly impact on the ability of the lid for its conformational heterogeneity as well as substrate release (38). From this, we extrapolated that the disfigurement of its substrate lid may be linked to the senescence-inducing property of murine mot-1 (16, 39) in contrast to the known lifespan-extending and immortalization features of mouse and human mot-2 (17–20). We initially tested whether or not mot-1 possesses a molecular chaperone activity. Although mot-2 showed chaperone properties, mot-1 showed low chaperone activity (35). Similarly, lidless variants of DnaK, which result in a lethal phenotype in yeasts (40), were

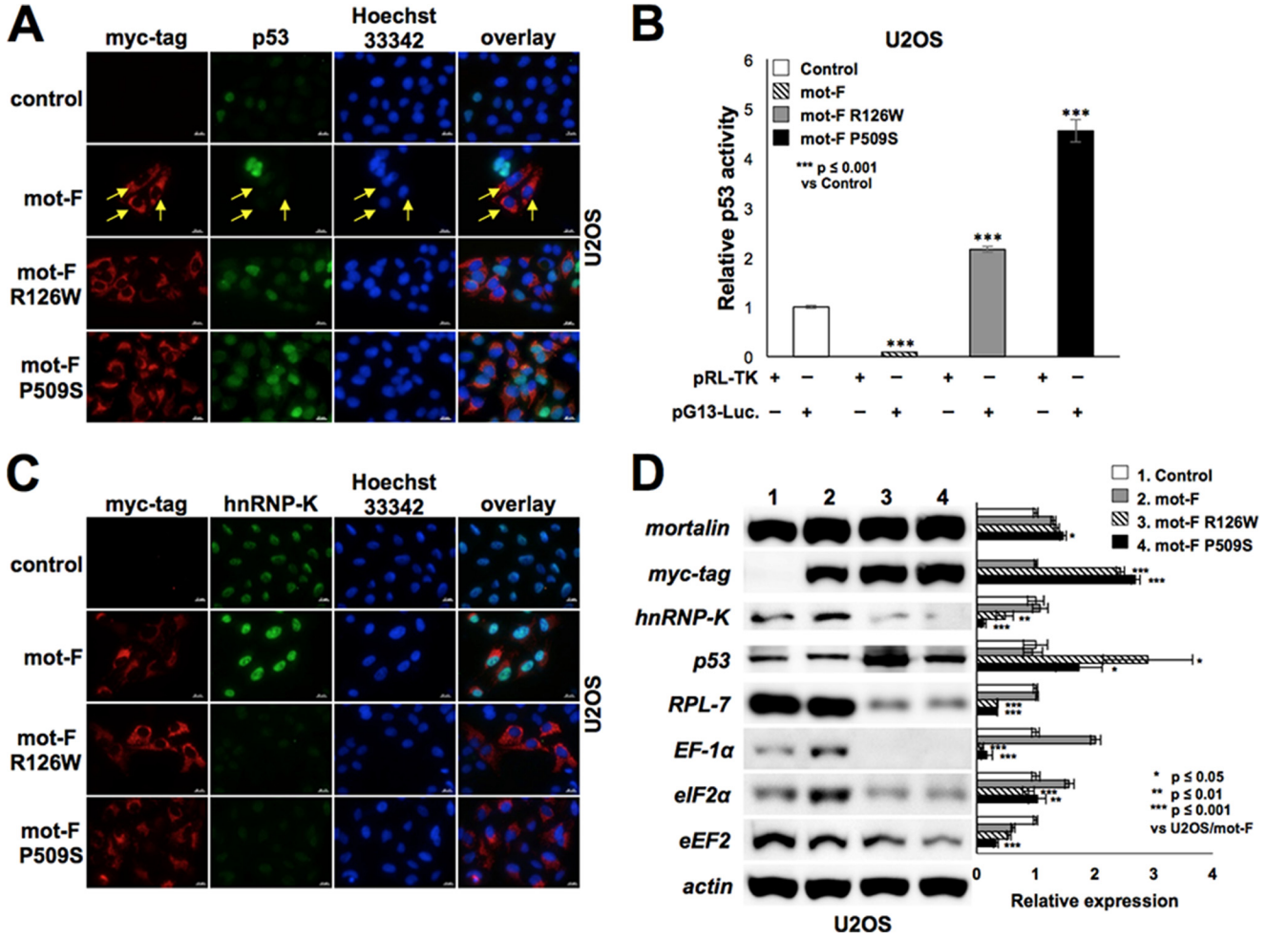

FIGURE 6. **Functional characterization of mortalin-PD mutants.** *A*, mot-PD mutants showing increase in nuclear p53 in contrast to mot-F-transduced cells, as indicated by *yellow arrows*. *B*, p53-dependent reporter activity increased in mot-PD-transduced cells in contrast to decrease in mot-F-transduced cells. *C*, mot-F-transduced cells show enhanced hnRNP-K protein in nucleus in contrast to its decrease in mot-PD cells. *D*, expression analysis of mot-PD mutant-transduced cells for the indicated proteins. Consistent with the immunostaining data, although p53 was found to be increased, the level of hnRNP-K decreased. RPL-7 and EF-1α (and its related proteins EF-2 and EF-2 α) showed decrease in mot-PD mutant-transduced cells. The data are expressed as a means $\pm$ S.E.

shown to lack chaperone activity (41). Similar defective chaperones also called "sick" chaperones have been implicated in several inherited diseases (42). Dominant negative mutants of α-crystalline (R116C) and α-B-crystalline (R120G) have been shown to lead to non-fatal congenital cataract and desmin-related myopathies, respectively (43).

RPL-7 belongs to the family of ribosomal proteins, highly conserved multifunctional proteins that serve as integral components of protein synthesis machinery and play a key role in regulation of DNA repair, cell growth, transformation, and death. It possesses a basic leucine zipper-like domain that endows it with a high-affinity binding capacity to mRNA/28 S rRNA and formation of homodimers (44). It is one of the few ribosomal proteins that, in addition to their presence in the cytoplasm, are also found in the nucleus, where they interact transiently or stably with RNA/DNA structures or other proteins. Several ribosomal proteins, including RPL11, RPL5, RPL23, RPS7, and RPS27L, have been shown to bind and inhibit MDM2, resulting in an activation of p53 tumor suppressor protein causing cell cycle arrest (45, 46). In contrast, some other ribosomal proteins, including RPL35a and RPS9, have been shown to be involved in deregulation of apoptosis and multi-drug resistance phenotype of cancer cells (47), suggesting their functions beyond ribosomal boundaries and in control of cell proliferation. Interestingly, RPL-7 was identified as a binding partner and regulator of vitamin D receptor (VDR) and retinoid X receptor (RXR)-mediated trans-activation (48), and mortalin was found to bind to retinoic acid receptor (RAR) and retinoid X receptor, where it plays an essential role in retinoic acid-induced neuronal differentiation (49).

EF-1α is another highly conserved ubiquitous protein involved in translation. It catalyzes the GTP-dependent binding of aminoacyl-transferase RNA (aa-tRNA) to ribosomes and regulates the rate and fidelity of polypeptide elongation. In addition, it has been shown to play a major role in the nuclear export of mRNA and proteins and to regulate the length and stability of microtubules, mitotic apparatus, and ribosomes (50). It is often enriched in tumors and has been positively correlated with cell growth and proliferation. Overexpression of EF-1α conferred protection against endoplasmic reticulum stress and apoptosis induced by growth factor withdrawal (51, 52). It was shown to interact with and inactivate p53 and p73 tumor suppressor proteins, resulting in chemoresistance (53). It also regulates phosphorylation of Akt/PKB, a serine/threo-

nine kinase involved in regulation of cell proliferation, survival, motility, and angiogenesis. Cells compromised for EF-1α showed decreased expression of phospho-Akt1 and phospho-Akt2 proteins, as well as reduced proliferation, survival, and invasion (54). Our data, described above, showed that the point mutations in mortalin caused (i) abrogation of its transforming activities mediated by inactivation of p53 and activation of hnRNP-K and telomerase, and (ii) caused severe decrease in RPL-7 and EF-1α proteins that are essential for translation and proliferation, suggesting that the wild-type mortalin plays a key role in stability and function(s) of these proteins. Furthermore, increase in endogenous oxidative stress and higher sensitivity to exogenous oxidative stress (Fig. 5) of mutant mortalin cells endorsed its role in stress protection. Lack of these functions resulted in premature senescence and Parkinson disease.

Taken together, the present study demonstrated, for the first time, the mechanism and functional significance of mortalin and its point mutations in control of cell proliferation with respect to carcinogenesis and premature aging.

Acknowledgments—We thank Drs. C. Deocaris, I. Kim, R. Singh, and N. Shah for their help.

REFERENCES

1. Muñoz-Espín, D., and Serrano, M. (2014) Cellular senescence: from physiology to pathology. *Nat. Rev. Mol. Cell Biol.* **15,** 482–496
2. Hayflick, L., and Moorhead, P. S. (1961) The serial cultivation of human diploid cell strains. *Exp. Cell Res.* **25,** 585–621
3. Campisi, J. (2005) Senescent cells, tumor suppression, and organismal aging: good citizens, bad neighbors. *Cell* **120,** 513–522
4. Cheung, C. T., Kaul, S. C., and Wadhwa, R. (2010) Molecular bridging of aging and cancer: a CARF link. *Ann. N.Y. Acad. Sci.* **1197,** 129–133
5. Hayflick, L. (1998) How and why we age. *Exp. Gerontol.* **33,** 639–653
6. Kaul, Z., Cesare, A. J., Huschtscha, L. I., Neumann, A. A., and Reddel, R. R. (2012) Five dysfunctional telomeres predict onset of senescence in human cells. *EMBO Rep.* **13,** 52–59
7. von Zglinicki, T. (2000) Role of oxidative stress in telomere length regulation and replicative senescence. *Ann. N.Y. Acad. Sci.* **908,** 99–110
8. Passos, J. F., Saretzki, G., von Zglinicki, T. (2007) DNA damage in telomeres and mitochondria during cellular senescence: is there a connection? *Nucleic Acids Res.* **35,** 7505–7513
9. Gaweda-Walerych, K., and Zekanowski, C. (2013) The impact of mitochondrial DNA and nuclear genes related to mitochondrial functioning on the risk of Parkinson's disease. *Curr. genomics* **14,** 543–559
10. Sõti, C., Sreedhar, A. S., and Csermely, P. (2003) Apoptosis, necrosis and cellular senescence: chaperone occupancy as a potential switch. *Aging Cell* **2,** 39–45
11. Shibata, Y., and Morimoto, R. I. (2014) How the nucleus copes with proteotoxic stress. *Curr. Biol.* **24,** R463-R474
12. Kaul, S. C., and Deocaris, C. C., and Wadhwa, R. (2007) Three faces of mortalin: a housekeeper, guardian and killer. *Exp. Gerontol.* **42,** 263–274
13. Soti, C., and Csermely, P. (2003) Aging and molecular chaperones. *Exp. Gerontol.* **38,** 1037–1040
14. Verbeke, P., Clark, B. F., and Rattan, S. I. (2001) Reduced levels of oxidized and glycoxidized proteins in human fibroblasts exposed to repeated mild heat shock during serial passaging *in vitro*. *Free Radic. Biol. Med.* **31,** 1593–1602
15. Wadhwa, R., Kaul, S. C., Ikawa, Y., and Sugimoto, Y. (1993) Identification of a novel member of mouse hsp70 family. Its association with cellular mortal phenotype. *J. Biol. Chem.* **268,** 6615–6621
16. Wadhwa, R., Kaul, S. C., Sugimoto, Y., and Mitsui, Y. (1993) Induction of cellular senescence by transfection of cytosolic mortalin cDNA in NIH 3T3 cells. *J. Biol. Chem.* **268,** 22239–22242
17. Kaul, S. C., Duncan, E. L., Englezou, A., Takano, S., Reddel, R. R., Mitsui, Y., and Wadhwa, R. (1998) Malignant transformation of NIH3T3 cells by overexpression of mot-2 protein. *Oncogene* **17,** 907–911
18. Kaul, S. C., Yaguchi, T., Taira, K., Reddel, R. R., and Wadhwa, R. (2003) Overexpressed mortalin (mot-2)/mthsp70/GRP75 and hTERT cooperate to extend the *in vitro* lifespan of human fibroblasts. *Exp. Cell Res.* **286,** 96–101
19. Yokoyama, K., Fukumoto, K., Murakami, T., Harada, S., Hosono, R., Wadhwa, R., Mitsui, Y., and Ohkuma, S. (2002) Extended longevity of *Caenorhabditis elegans* by knocking in extra copies of hsp70F, a homolog of mot-2 (mortalin)/mthsp70/Grp75. *FEBS Lett.* **516,** 53–57
20. Wadhwa, R., Takano, S., Robert, M., Yoshida, A., Nomura, H., Reddel, R. R., Mitsui, Y., Kaul, S. C. (1998) Inactivation of tumor suppressor p53 by mot-2, a hsp70 family member. *J. Biol. Chem.* **273,** 29586–29591
21. Kaul, S. C., Takano, S., Reddel, R. R., Mitsui, Y., and Wadhwa, R. (2000) Transcriptional inactivation of p53 by deletions and single amino acid changes in mouse mot-1 protein. *Biochem. Biophys. Res. Commun.* **279,** 602–606
22. Ma, Z., Izumi, H., Kanai, M., Kabuyama, Y., Ahn, N. G., and Fukasawa, K. (2006) Mortalin controls centrosome duplication via modulating centrosomal localization of p53. *Oncogene* **25,** 5377–5390
23. Lu, W. J., Lee, N. P., Kaul, S. C., Lan, F., Poon, R. T., Wadhwa, R., and Luk, J. M. (2011) Mortalin-p53 interaction in cancer cells is stress dependent and constitutes a selective target for cancer therapy. *Cell Death Differ.* **18,** 1046–1056
24. Lu, W. J., Lee, N. P., Kaul, S. C., Lan, F., Poon, R. T., Wadhwa, R., and Luk, J. M. (2011) Induction of mutant p53-dependent apoptosis in human hepatocellular carcinoma by targeting stress protein mortalin. *Int. J. Cancer* **129,** 1806–1814
25. Yang, L., Guo, W., Zhang, Q., Li, H., Liu, X., Yang, Y., Zuo, J., and Liu, W. (2011) Crosstalk between Raf/MEK/ERK and PI3K/AKT in suppression of Bax conformational change by Grp75 under glucose deprivation conditions. *J. Mol. Biol.* **414,** 654–666
26. Ryu, J., Kaul, Z., Yoon, A. R., Liu, Y., Yaguchi, T., Na, Y., Ahn, H. M., Gao, R., Choi, I. K., Yun, C. O., Kaul, S. C., and Wadhwa, R. (2014) Identification and functional characterization of nuclear mortalin in human carcinogenesis. *J. Biol. Chem.* **289,** 24832–24844
27. Tai-Nagara, I., Matsuoka, S., Ariga, H., and Suda, T. (2014) Mortalin and DJ-1 coordinately regulate hematopoietic stem cell function through the control of oxidative stress. *Blood* **123,** 41–50
28. Qu, M., Zhou, Z., Chen, C., Li, M., Pei, L., Yang, J., Wang, Y., Li, L., Liu, C., Zhang, G., Yu, Z., and Wang, D. (2012) Inhibition of mitochondrial permeability transition pore opening is involved in the protective effects of mortalin overexpression against β-amyloid-induced apoptosis in SH-SY5Y cells. *Neurosci. Res.* **72,** 94–102
29. Banerjee, S., and Chinthapalli, B. (2014) A proteomic screen with *Drosophila* Opa1-like identifies Hsc70–5/Mortalin as a regulator of mitochondrial morphology and cellular homeostasis. *Int. J. Biochem. Cell Biol.* **54,** 36–48
30. Park, S. J., Shin, J. H., Jeong, J. I., Song, J. H., Jo, Y. K., Kim, E. S., Lee, E. H., Hwang, J. J., Lee, E. K., Chung, S. J., Koh, J. Y., Jo, D. G., and Cho, D. H. (2014) Down-regulation of mortalin exacerbates Aβ-mediated mitochondrial fragmentation and dysfunction. *J. Biol. Chem.* **289,** 2195–2204
31. Burbulla, L. F., Fitzgerald, J. C., Stegen, K., Westermeier, J., Thost, A. K., Kato, H., Mokranjac, D., Sauerwald, J., Martins, L. M., Woitalla, D., Rapaport, D., Riess, O., Proikas-Cezanne, T., Rasse, T. M., and Krüger, R. (2014) Mitochondrial proteolytic stress induced by loss of mortalin function is rescued by Parkin and PINK1. *Cell Death Dis.* **5,** e1180
32. De Mena, L., Coto, E., Sánchez-Ferrero, E., Ribacoba, R., Guisasola, L. M., Salvador, C., Blázquez, M., and Alvarez, V. (2009) Mutational screening of the mortalin gene (HSPA9) in Parkinson's disease. *J. Neural. Transm.* **116,** 1289–1293
33. Zhu, J. Y., Vereshchagina, N., Sreekumar, V., Burbulla, L. F., Costa, A. C., Daub, K. J., Woitalla, D., Martins, L. M., Krüger, R., and Rasse, T. M. (2013) Knockdown of Hsc70–5/mortalin induces loss of synaptic mitochondria in a *Drosophila* Parkinson's disease model. *PLoS One* **8,** e83714
34. Kaul, S. C., Aida, S., Yaguchi, T., Kaur, K., and Wadhwa, R. (2005) Activation of wild type p53 function by its mortalin-binding cytoplasmically

localizing carboxy-terminus peptides. *J. Biol. Chem.* **280,** 39373–39379
35. Deocaris, C. C., Yamasaki, K., Kaul, S. C., and Wadhwa, R. (2006) Structural and functional differences between mouse mot-1 and mot-2 proteins that differ in two amino acids. *Ann. N.Y. Acad. Sci.* **1067,** 220–223
36. Burbulla, L. F., Schelling, C., Kato, H., Rapaport, D., Woitalla, D., Schiesling, C., Schulte, C., Sharma, M., Illig, T., Bauer, P., Jung, S., Nordheim, A., Schöls, L., Riess, O., and Krüger, R. (2010) Dissecting the role of the mitochondrial chaperone mortalin in Parkinson's disease: functional impact of disease-related variants on mitochondrial homeostasis. *Hum. Mol. Genet.* **19,** 4437–4452
37. Schmid, D., Baici, A., Gehring, H., and Christen, P. (1994) Kinetics of molecular chaperone action. *Science* **263,** 971–973
38. Slepenkov, S. V., Patchen, B., Peterson, K. M., and Witt, S. N. (2003) Importance of the D and E helices of the molecular chaperone DnaK for ATP binding and substrate release. *Biochemistry* **42,** 5867–5876
39. Nakabayashi, K., Ogata, T., Fujii, M., Tahara, H., Ide, T., Wadhwa, R., Kaul, S. C., Mitsui, Y., and Ayusawa, D. (1997) Decrease in amplified telomeric sequences and induction of senescence markers by introduction of human chromosome 7 or its segments in SUSM-1. *Exp. Cell Res.* **235,** 345–353
40. Strub, A., Zufall, N., and Voos, W. (2003) The putative helical lid of the Hsp70 peptide-binding domain is required for efficient preprotein translocation into mitochondria. *J. Mol. Biol.* **334,** 1087–1099
41. Buczynski, G., Slepenkov, S. V., Sehorn, M. G., and Witt, S. N. (2001) Characterization of a lidless form of the molecular chaperone DnaK: deletion of the lid increases peptide on- and off-rate constants. *J. Biol. Chem.* **276,** 27231–27236
42. Giffard, R. G., Macario, A. J., de Macario, E. C. (2013) The future of molecular chaperones and beyond. *J. Clin. Invest.* **123,** 3206–3208
43. Vicart, P., Caron, A., Guicheney, P., Li, Z., Prévost, M. C., Faure, A., Chateau, D., Chapon, F., Tomé, F., Dupret, J. M., Paulin, D., and Fardeau, M. (1998) A missense mutation in the αB-crystallin chaperone gene causes a desmin-related myopathy. *Nat. Genet.* **20,** 92–95
44. Hemmerich, P., von Mikecz, A., Neumann, F., Sözeri, O., Wolff-Vorbeck, G., Zoebelein, R., and Krawinkel, U. (1993) Structural and functional properties of ribosomal protein L7 from humans and rodents. *Nucleic Acids Res.* **21,** 223–231
45. Dai, M. S., Shi, D., Jin, Y., Sun, X. X., Zhang, Y., Grossman, S. R., and Lu, H. (2006) Regulation of the MDM2-p53 pathway by ribosomal protein L11 involves a post-ubiquitination mechanism. *J. Biol. Chem.* **281,** 24304–24313
46. Dai, M. S., Challagundla, K. B., Sun, X. X., Palam, L. R., Zeng, S. X., Wek, R. C., and Lu, H. (2012) Physical and functional interaction between ribosomal protein L11 and the tumor suppressor ARF. *J. Biol. Chem.* **287,** 17120–17129
47. Shi, Y., Zhai, H., Wang, X., Han, Z., Liu, C., Lan, M., Du, J., Guo, C., Zhang, Y., Wu, K., and Fan, D. (2004) Ribosomal proteins S13 and L23 promote multidrug resistance in gastric cancer cells by suppressing drug-induced apoptosis. *Exp. Cell Res.* **296,** 337–346
48. Berghöfer-Hochheimer, Y., Zurek, C., Wölfl, S., Hemmerich, P., and Munder, T. (1998) L7 protein is a coregulator of vitamin D receptor-retinoid X receptor-mediated transactivation. *J. Cell. Biochem.* **69,** 1–12
49. Shih, Y. Y., Lee, H., Nakagawara, A., Juan, H. F., Jeng, Y. M., Tsay, Y. G., Lin, D. T., Hsieh, F. J., Pan, C. Y., Hsu, W. M., and Liao, Y. F. (2011) Nuclear GRP75 binds retinoic acid receptors to promote neuronal differentiation of neuroblastoma. *PLoS One* **6,** e26236
50. Condeelis, J. (1995) Elongation factor 1 α, translation and the cytoskeleton. *Trends Biochem. Sci.* **20,** 169–170
51. Grant, A. G., Flomen, R. M., Tizard, M. L., and Grant, D. A. (1992) Differential screening of a human pancreatic adenocarcinoma λ gt11 expression library has identified increased transcription of elongation factor EF-1α in tumour cells. *Int. J. Cancer* **50,** 740–745
52. Talapatra, S., Wagner, J. D., and Thompson, C. B. (2002) Elongation factor-1 α is a selective regulator of growth factor withdrawal and ER stress-induced apoptosis. *Cell Death Differ.* **9,** 856–861
53. Blanch, A., Robinson, F., Watson, I. R., Cheng, L. S., and Irwin, M. S. (2013) Eukaryotic translation elongation factor 1-α1 inhibits p53 and p73 dependent apoptosis and chemotherapy sensitivity. *PLoS One* **8,** e66436
54. Pecorari, L., Marin, O., Silvestri, C., Candini, O., Rossi, E., Guerzoni, C., Cattelani, S., Mariani, S. A., Corradini, F., Ferrari-Amorotti, G., Cortesi, L., Bussolari, R., Raschellà, G., Federico, M. R., and Calabretta, B. (2009) Elongation factor 1 α interacts with phospho-Akt in breast cancer cells and regulates their proliferation, survival and motility. *Mol. Cancer* **8,** 58